

## NOVEL MODELING AND DESIGN OF CIRCULARLY POLARIZED DIELECTRIC RESONATOR ANTENNA ARRAY

M. F. Ain<sup>1,\*</sup>, Y. M. Qasaymeh<sup>1</sup>, Z. A. Ahmad<sup>2</sup>,  
M. A. Zakariya<sup>1</sup>, M. A. Othman<sup>1</sup>, S. S. Olokede<sup>1</sup>,  
and M. Z. Abdullah<sup>1</sup>

<sup>1</sup>School of Electrical and Electronic Engineering, Universiti Sains Malaysia, Malaysia

<sup>2</sup>School of Materials and Mineral Resources Engineering, Universiti Sains Malaysia, Malaysia

**Abstract**—This paper presents a design of circularly polarized dielectric resonator antenna (DRA) array. The dielectric resonators (DRs) were excited by rectangular aperture coupling slots feed with a linear microstrip. The slot positions were determined based on the characteristic of standing wave ratio over a short ended microstrip to deliver the maximum amount of coupling power to the DRs, in order to improve the array gain. Each DR element was rotated 45° with respect to the sides of the exciting slot to generate circular polarization pattern. The DRA array was modeled and simulated as a parallel RLC input impedance component using Agilent (ADS) software, since that will ensure the resonant frequency of the antenna as primary design step before simulating in (CST) software and doing the measurements. The results of the return loss, gain radiation and pattern axial ratio are shown. The gain of the proposed array in X band was about 8.5 dBi, while the 3 dB axial ratio bandwidth started from 8.14 to 8.24 GHz. The impedance bandwidths started from 8.14 GHz to 8.26 GHz. The proposed DRA exhibited an enhancement of the gain in comparison to a single pellet DRA. The size of the whole antenna structure is about 40 mm × 50 mm and can potentially be used in wireless systems.

### 1. INTRODUCTION

Since first introduced by Long et al. [1] in 1983, the dielectric resonator antenna (DRA) has received increasing attention in the last two

---

*Received 18 February 2012, Accepted 2 April 2012, Scheduled 10 April 2012*

\* Corresponding author: Mohd Fadzil Ain (mfadzil@eng.usm.my).

decades. The DRA has many advantages such as its small size, light weight, wide bandwidth, high radiation efficiency, low cost, low loss, and excitation of surface waves. It also has an advantage over the microstrip antenna in that the former has a wider impedance bandwidth. Different shapes of DRA have been presented on the literature. The rectangular DR offers practical advantages such as they have more design flexibility.

DRA's are normally low-gain antennas with a broad radiation pattern. As with other traditional low-gain antennas, DRA's can be arrayed to obtain a higher gain. Several types of feeding have been used to feed a linear array of DRA's to achieve this objective, such as microstrip lines [2], coplanar waveguide [3], slotted waveguide [4], and dielectric image line [5]. Among these excitation schemes, aperture coupling with a microstrip feed line is most frequently used because of ease of fabrication, compatibility with MMIC, and the isolation between the antenna and the feeding network [6].

Several CP DRA's techniques have been introduced in the literature. By varying the length to width ratio and with suitable excitation, two degenerate modes with  $90^\circ$  phase differences can be excited in the DRA, resulting in circular polarization [7, 8]. If a rectangular DRA excited by a narrow rectangular slot positioning  $45^\circ$  with respect to the sides produces circular polarization. Some other circular polarization DRA's techniques were reported, which use a quadrature feed [9], Single feed [10, 11], a parasitic patch placed on top of a rectangular DRA [12, 13], or designing a cross-shaped DRA [14]. Recently, the elliptical CP DRA's was introduced [8]. Other techniques used a geometrically modified rectangular DRA [15] while sequential rotation sub-arrays of circularly polarized or linearly polarized antenna elements have been introduced to enhance the CP AR bandwidth [16].

However, circularly polarized (CP) antennas are more preferable than linear polarized (LP) antennas in some applications, such as radar systems and satellite communications. Few circularly polarized DRA arrays were reported in the literature. Pang et al. (2000) [17] introduced four CP cylindrical DRA's with cross-slot coupling of unequal slot lengths and a sequentially rotated microstrip feed which demonstrated that left-hand CP (LHCP) could be realized. An array based on geometrically modified rectangular DRA's was also demonstrated by Haneishi and Takazawa (1985) [18]. The 16 element array with paired units was designed to operate at X-band frequencies. The DRA's were fed using 16-way microstrip power dividers mounted on the rear panel of the array. A broadside axial ratio of less than 1 dB over the frequency range between 9.5 GHz and 10 GHz was also obtained. A four-element CP cross-DRA (XDRA) array was reported

by Petosa et al. (1996) [19]. The XDRAs were coupled by single slots together with a microstrip feed, with the arms of the XDRAs rotated at  $45^\circ$  with respect to the length of the slot. The XDRA elements were sequentially rotated so as to increase the CP bandwidth. The array operated at 11.5 GHz with a 3 dB axial ratio bandwidth of 16% over a beamwidth of 400, and a 10 dB return loss bandwidth of 25%. Kejani and Neshati (2010) [20] introduced a linear circular polarized (CP) Dielectric Resonator Antenna (DRA) array which consisted of 3-element DRA using elliptical resonators and positioned on top of a metallic ground plane exciting through narrow slots. The gain obtained by the array was 3 dB more than the gain obtained by the array with a single element at 10 GHz. The CP arrays formed using CP DRA elements give better performance in terms of 3 dB axial ratio bandwidth, gain and 3 dB-gain bandwidth [19].

The purpose of this paper is three folds, first to enhance the gain second to acquire circular polarization and third introducing a new method for calculating the dimensions of rectangular DR fed by microstrip slot coupled based on their impedance model. The gain can be effectively improved through the use of the standing wave ratio over microstrip short ended characteristic. The circular polarization was obtained by rotating each DRA element to obtain  $45^\circ$  with the respect to the slot sides. This is the easiest way to acquire CP radiation compared to CP DRA arrays which were reported to use cross-slots, geometrically modified rectangular DRAs and elliptical resonators. Coupling slots were used since the radiation being essentially emitted by the DRA only and it is the most suitable for large DRA arrays where relatively simple circuit integration is required as compared to other feeding mechanisms. Moreover, the ground plane effectively isolates any fields or currents inherent in the feed network from affecting the radiation pattern of the radiating element. It was shown that the gain can be effectively improved through the use of the standing wave ratio over microstrip short ended characteristic. Characteristics were mainly those of the DR.

In Section 2, the configuration of feeding method and spacing between DRs will be explained. The dimensions of DRA array elements and their relative impedances will be calculated in Section 3. In Section 4, the results for  $S_{11}$ , radiation pattern, axial ratio and gain will be presented.

## 2. CONFIGURATION OF FEEDING METHOD

The DRA was excited with a 50-microstrip feeder with a width of 1.7 mm, designed on a RO4003C microwave substrate with  $\epsilon_s$  of 3.38

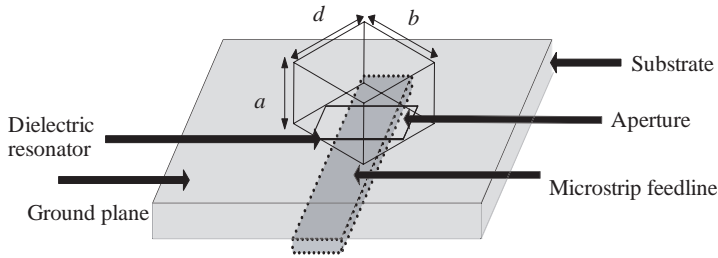


**Figure 1.** Rectangular slot coupled with dielectric element making  $45^\circ$  with slot sides for CP radiation. [22].

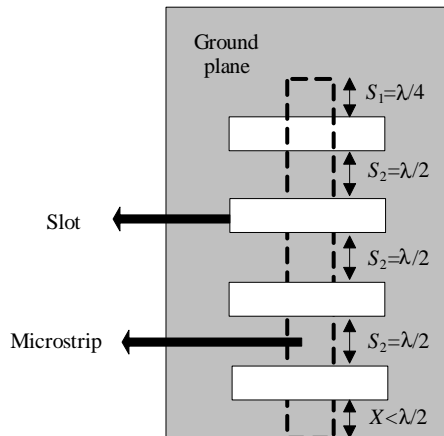


**Figure 2.** The designed array showing the spacing between the elements (dielectric elements located on the coupling slots were omitted).

and a thickness of 0.813 mm. The CCTO ( $\text{CaCu}_3\text{Ti}_4\text{O}_{12}$ ) material with a dielectric constant  $\epsilon_r = 55$  was used as a resonator. The microstrip fed aperture coupled patch antennas were first used in 1985 [21]. This technique has seen extensive use for both microstrip patch and DRA applications. With the advantage of easy integration with MIC component and effective use at high frequencies, this method is very popular. A simple representation is shown in Figure 1. Typically, a radiating dielectric element is placed over the slot. A microstrip transmission line on top of the substrate is electromagnetically coupled, through an aperture in the common ground plane, to the dielectric resonator antenna.

The quarter-wavelength shorted stub is a special case of the stub

concept that finds particular application in microwave circuits. The feed line is terminated by a quarter-wavelength short-ended stub to maximize the amount of power coupled to the antenna [23, 24]. The stub lengthening  $S$  is picked out so that its reactance cancels out that of the slot window. This is typically chosen to be:

$$S = \frac{\lambda_g}{4} \quad (1)$$

where  $\lambda_g$  is the guided wave length.

Figure 2 indicates the voltage allocation over the length of the line when the load end of the microstrip line is shorted. The same impedance and voltage condition is periodic every half-wavelength further down the line from the load completion toward the generator. Voltage minima are called nodes, and voltage maxima are called antinodes. The antenna configuration consisted of a microstrip line on the front plane and three coupling slots on the ground plane while the DRs were positioned over the slots. The first slot was positioned a quarter-wavelength from the microstrip end and since the antinodes would repeat itself every half wavelength along the shorted microstrip line after the first antinode, the next two coupling slots were positioned every half wavelength (the second slot positioned a half wave length apart from the first one and the third another half wave length from the second) toward the source to achieve maximum amount of coupling in order to maximize the radiation of the DRs. DRs located over the coupling slots are omitted to better visualize the coupling technique.  $S_1$  equals to quarter wave length which represents the last element of the array.  $S_2$  is the distance that separates the elements which equals to half wave length, while,  $X$  is the distance from the source to the first element which is less than half wavelength and prevents more antinodes along the microstrip. Since the slot radiates in both directions, backward and forward, a reflector will be inserted above the microstrip to decrease the back radiation of the antenna.

### 3. DIMENSIONS AND MODELING OF DRA ARRAY

The aim of analyzing the input impedance of the proposed array is to determine the dimensions of the each rectangular DRs in an iterative manner, normally the dimensions of the individual rectangular DRs are determined using the equations in [25] also in an iterative manner. An equivalent circuit model was postulated to describe and enable one to quantify the values of the individual resonant frequencies antenna array elements. An equivalent circuit, which describes such a resonance for single DR, is shown in Figure 3. The entire model consists of Four resonant circuits with resonant frequencies  $f_{01}$ ,  $f_{02}$ ,  $f_{03}$  and  $f_{04}$ .

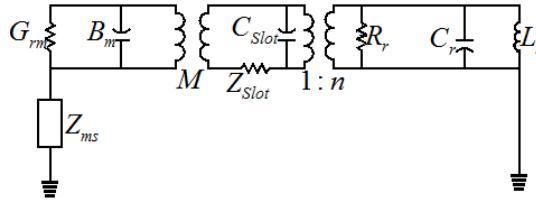


**Figure 3.** Equivalent circuit of microstrip slot coupled single DR.

A procedure presented to give a physical insight into the wideband behavior of the antenna is described in [26, 27].

The first step is to model the DR with a RLC network. The formulas to represent a resonator as a parallel resonant circuit can be found in [28, 29] when the resonator is coupled to the excitation source.

$$R_r = \frac{2n^2 z_0 s_{11}}{1 - s_{11}}, \quad (2a)$$

$$C_r = \frac{Q_0}{\omega_0 R_r}, \quad (2b)$$

$$L_r = \frac{1}{C_r \omega_0}. \quad (2c)$$

where

$s_{11}$  The reflection coefficient.

$z_0$  The characteristic impedance.

$Q_0$  The quality factor.

$n$  Represent the coupling magnitude between the DR and the excitation source.

It is mentioned in [28] that the value of  $R_r$  can be chosen. Since the value of  $R_r$  plays an important role in determining values of  $C_r$  and  $L_r$ , finding a suitable  $R_r$  value is a more complicated process in order to achieve reasonable  $C_r$  and  $L_r$ . Thus, an Agilent advanced design system (ADS) program has been used to extract the optimum values of RLC, while a Matlab<sup>®</sup> program has been developed to analyze values of RLC which will be used to determine the dimensions of DRs. The factor  $n$  in Equation (2a) represents the coupling magnitude between the DR and excitation source (slot in this case) which plays an important role to determine  $R_r$  and, later on,  $C_r$ ,  $L_r$ .

The second step is to find the input impedance of the slot. When the transmission line is terminated by a stub length  $\lambda_g/4$  (i.e., antinode), the input impedance is simply put under the infinite line assumption and this result is added as series reactance,  $X =$

$-jZ_c \cot(\beta_f L_t)$ . The total impedance is then:

$$Z_{Slot} = Z_c \frac{2R}{1-R} + X = Z_c \frac{2R}{1-R} + jZ_c \cot(\beta_f L_t) \quad (3)$$

where:

$Z_c$  Characteristic impedance of transmission line.

$R$  Voltage reflection coefficient.

$\beta_f$  Propagation constant.

$L_t$  Stub length.

$Z_{Slot}$  Can be calculated using program in [30].

The third step is to find the input impedance of the microstrip line. At the antinodes points, the input impedance is high resistance, hence the line acts as a parallel resonant circuit. As in [31], the input admittance  $Y_m$  is equal to  $G_{rm} + jB_m$  where  $G_{rm}$  is the equivalent radiation conductance and  $B_m$  is the susceptance of the fringing field capacitance of the microstrip. The expressions of  $G_{rm}$  and  $B_m$  are:

$$G_{rm} = \frac{160\pi^2 h^2}{Z_{cm}^2 \lambda_0^2 \epsilon_{cm}} \quad (4a)$$

$$B_m = \omega C_l, \quad C_l = \frac{l_{eq} C \sqrt{\epsilon_{cm}}}{Z_{cm}} \quad (4b)$$

where:

$h$  Substrate height.

$Z_{cm}$  Characteristic impedance of the microstrip.

$\epsilon_{cm}$  Effective dielectric constant.

$l_{eq}$  Equivalent extra length of microstrip.

$C$  Velocity of light.

The last step is to transform the impedance of the slot along the microstrip line. The mutual inductance between the microstrip and the slot is:

$$M = (\mu_0 W_s / 2\pi) \ln(\sec \theta_0), \quad \theta_0 = \arctan(L_s / 2h) \quad (5)$$

where

$W_s$  The slot width.

$L_s$  The slot length.

$h$  The substrate height.

$\mu_0$  Permeability of free space.

Every antenna impedance function has an equivalent circuit in Darlington form. The dimensions of the slots were assumed and their relative impedances were calculated using Equation (3). The impedance of the  $50\Omega$  microstrip was calculated from Equations (4a), (4b). Four stage circuit as in Figure 3 was built in ADS representing the entire array including the uncalculated values of the

parallel RLC representing the three DRs. With the help of ADS, the three parallel RLC will be tuned to resonate at the desired frequency, and then a Matlab<sup>®</sup> program based on Equations (2a), (2b), (2c) will be used to extract the dimensions of each DR according to its resonant frequency. No wideband operation is expected in this stage since the model doesn't include the mutual coupling between the DRs. Once the input impedance model success, the antenna will be modeled in (CST). Measurements for return loss, radiation pattern, and gain compared with those results achieved from CST will be the final step in the design.

#### 4. RESULTS AND DISCUSSIONS

By solving Equation (1) for frequency equals to 8.5 GHz, the quarter wavelength ( $S_1$ ) equals to 5.41 mm and the half wavelength ( $S_2$ ) equals to 10.82 mm, while the  $X$  is set to be 4 mm in order to obtain no more antinodes along the feeder. Figure 5 shows the simulated power radiation antinodes over the microstrip using CST software. It was clear that the antinodes took their places at approximately the positions which were calculated by solving Equation (1) at 8.5 GHz. As can be seen in Figure 4, the slots were placed to take their positions on the antinodes, while the DRA elements were placed over the coupling slots.

Then, by solving Equations (2a), (2b), (2c), the dimensions of the DRs were found to be 5 mm (width), 5 mm (length), and 2 mm (height), for the first and last elements, and 6 mm (width), 6 mm (length), and 2 mm (height), for the middle element.

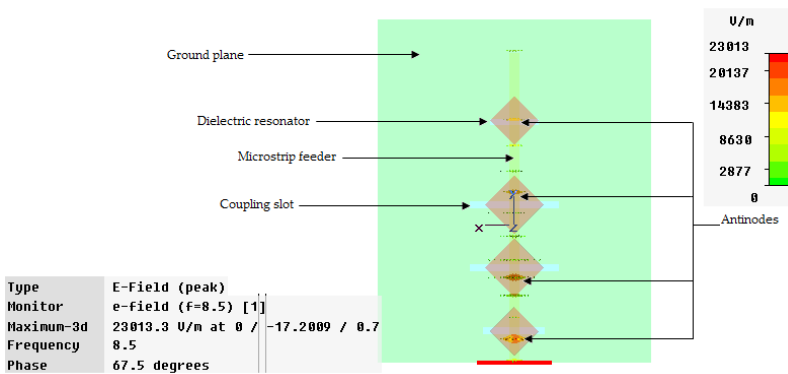


**Figure 4.** The maximum power radiated antinodes over the microstrip at 8.5 GHz from CST.

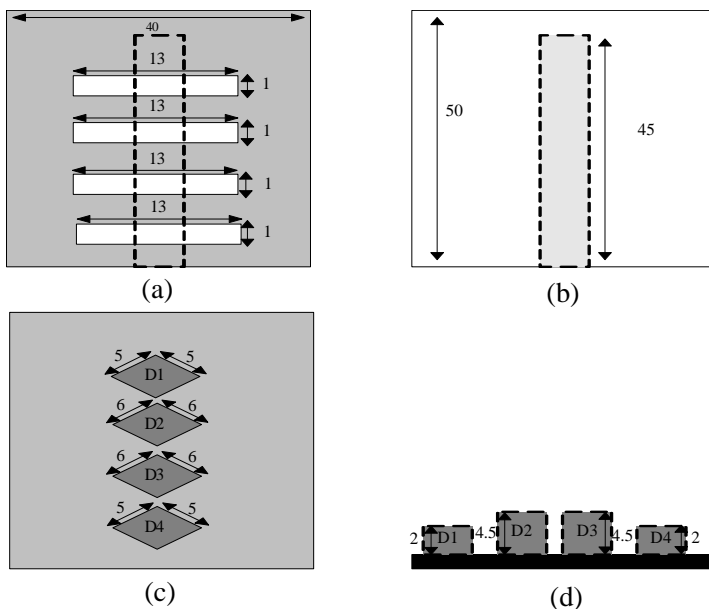


**Figure 5.** The designed structure in CST, (a) slots dimensions (width of the slots = 1 mm) (dielectric omitted), (b) microstrip dimensions (width = 1.7 mm), (c) dielectrics lengths and widths (slots omitted), and (d) dielectric elements heights.

4.5 mm (height) for the third and fourth elements, respectively. The aim of this difference in DR dimensions was for acquiring directive radiation pattern. The dimensions of the slots were set to be 13 mm in length and 1 mm in width. The dimensions of the proposed array are shown in Figure 5.

For modeling the array elements into the equivalent impedance circuit using Agilent advanced design system (ADS), the impedances of the microstrip, slot, DR and coupling between them can be calculated using Equations (6), (8a), (8b), (9) and (10) mentioned in Section 3. Since the value of  $R_r$  plays a role in determining  $C_r$  and  $L_r$ , 55 Ohm was chosen because reasonable and realistic  $C_r$  and  $L_r$  values can be achieved. The aim of this model is to ensure that the proposed antenna will resonate at the desired frequency as an initial design step once that achieved the modeling in CST and measurements will be done. The values of input impedances of the microstrip slots and DRs are shown in Figure 6.

The simulation and measurement results for the input return loss are given in Figure 7. The simulated return loss model in ADS was

-14.86 dB at 8.5 GHz and that proves the antenna resonating at the designed frequency. The minimum CST simulated input return loss frequency could be fine tuned to 8.445 GHz equals to -13.9 dB with a bandwidth of 17.66 MHz and impedance of  $52.23 - j4.55 \Omega$ . The minimum measured input return loss is 8.46 GHz of -16 dB and a bandwidth of 42 MHz and impedance of  $51.23 + j13 \Omega$ .

Figure 8 shows the simulated and measured gain of the antenna at a frequency range of 8.43 GHz to 8.45 GHz. The maximum simulated gain obtained from CST was 8.63 dBi at 8.45 GHz. The maximum measured gain was 8.51 dBi at 8.45 GHz, compared to the standard

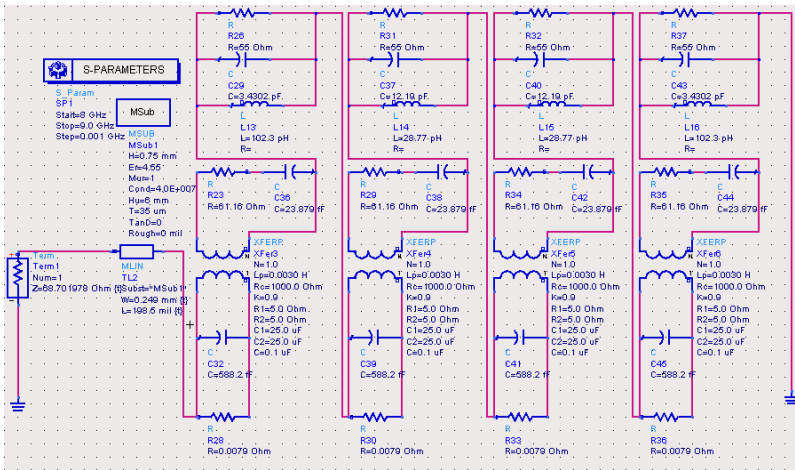


Figure 6. The dielectric resonator antenna array model in ADS.

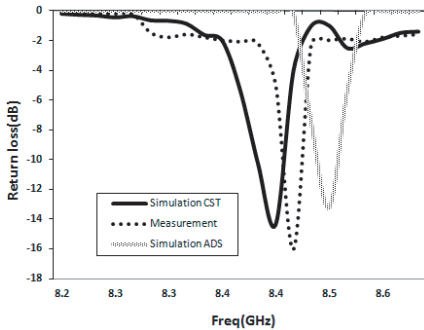


Figure 7. The measured and simulated return loss.

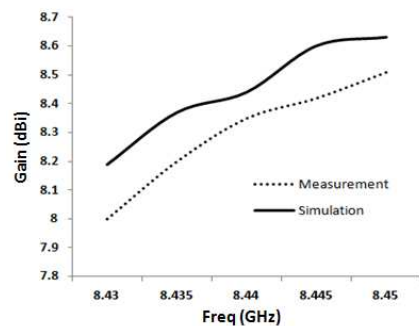


Figure 8. The measured and simulated gain.

Helix antennas using gain absolute methods by using the network analyzer to measure the  $S_{21}$  of the designed DRA array and compare it to the  $S_{21}$  measured for the standard known gain antenna. The array shows a gain improvement since the antenna gain of a single DRA is limited to about 5 dBi. It indicates that this antenna has high efficiency with minimum loss. This is because there is no conductor loss in the DR. However, conductor loss exists in the microstrip line but is very small.

Figure 9 shows the simulated and measured co-polarization and cross-polarization patterns in the  $xz$ -plane at 8.45 GHz. The cross-polarization is lower than co-polarization by 20 dB in the broadside direction in measurement, which is the characteristic of right hand circular polarization (RHCP) radiation. Simulation results also

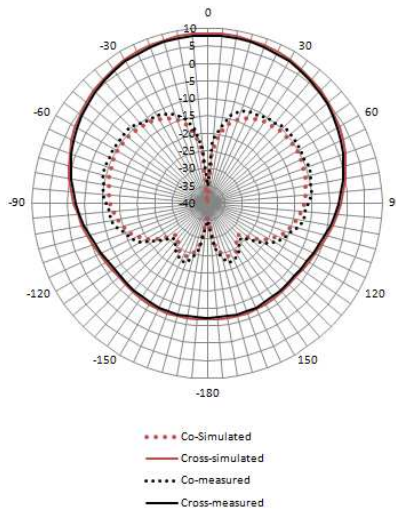


Figure 9. Radiation patterns of the CP DRA array at 8.45 GHz.

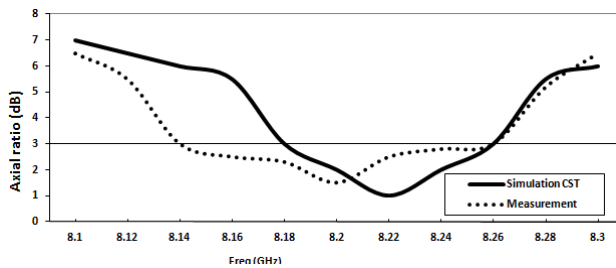


Figure 10. Measured and simulated 3 dB axial ratio.

show good agreement with those measured radiation patterns values achieved using the spectrum analyzer as a receiver. The difference between simulated and measured values is slightly small and since the data plotting in Figure 9 ranges from  $-40$  dB to  $10$  dB makes them both quite having the same values. Roughly the same records in gain and radiation pattern measurement were achieved even the measurements set up were different. The difference between simulation and measurement is clearer in Figure 8 rather than Figure 9 due to plotting step range.

Figure 10 shows the corresponding axial ratio. The AR is measured with a linear standard gain monopole antenna. The AR is found by measuring the fields  $E\theta$  and  $E\phi$  in the vertical and horizontal plane. The measured 3 dB AR bandwidth of the proposed antenna is from  $8.18$  to  $8.26$  GHz while the measured 3 dB AR bandwidth of the proposed antenna is from  $8.14$  to  $8.26$  GHz.

**Table 1.** Comparison of carried out work with reported literature.

Published work	C.P. Technique	Frequency band	Gain	Feeding method
Pang et al. (2000)	Cross slot coupling	C-band	12 dBi	Microstrip slot coupling (sequential rotation)
Haneishi and Takazawa (1985)	Modified rectangular DRA	X-band	Not mentioned	Microstrip (sequential rotation)
Kejani and Neshati (2010)	Elliptical resonators	X-band	9 dBi	Dielectric image line (slot coupled)
Petosa (1996)	Cross-shaped DRA	X-band	Not mentioned	Microstrip slot coupling (sequential rotation)
<b>Proposed work</b>	<b>Rectangular DR rotated <math>45^\circ</math> with a rectangular slot</b>	<b>X-band</b>	<b>9 dBi</b>	<b>Microstrip series fed (slot coupled)</b>

## 5. CONCLUSION

In this paper, a new feeding and modeling method for high gain CP DRA array at X band is presented. The proposed arrays are fed by a microstrip slot coupled structure employing the characteristic of short ended microstrip line. Good high gain CP performance was obtained compared to single element DRA. Reasonable agreement between simulated and measured data was obtained. A noticed reduction of the size of the array compared with designed reported in the literature. Table 1 shows a comparison between reported CP DRA arrays and the array presented in this paper.

## ACKNOWLEDGMENT

The authors gratefully acknowledge that this work was financially supported by the FRGS grant under project number 203/PELECT/6071183 and RUT grant number 1001/PELECT/854004.

## REFERENCES

1. Long, S., M. McAllister, and S. Liang, "The resonant cylindrical dielectric cavity antenna," *IEEE Transactions on Antennas and Propagation*, Vol. 31, No. 2, 406–412, 1983.
2. Wee, F. H., et al., "Investigation of the characteristics of barium strontium titanate (BST) dielectric resonator ceramic loaded on array antennas," *Progress In Electromagnetics Research*, Vol. 121, 181–213, 2011.
3. Lee, R. Q. and R. N. Simons, "Bandwidth enhancement of dielectric resonator antennas," *1993 Digest, Antennas and Propagation Society International Symposium, AP-S*, 1993.
4. Eshrah, I. A., et al., "Theory and implementation of dielectric resonator antenna excited by a waveguide slot," *IEEE Transactions on Antennas and Propagation*, Vol. 53, No. 1, 483–494, 2005.
5. Al-Zoubi, A. S., A. A. Kishk, and A. W. Glisson, "Analysis and design of a rectangular dielectric resonator antenna fed by dielectric image line through narrow slots," *Progress In Electromagnetics Research*, Vol. 77, 379–390, 2007.
6. Ain, M. F., Y. M. Qasaymeh, Z. A. Ahmad, M. A. Zakariya, M. A. Othman, A. A. Sulaiman, A. Othman, S. D. Hutagalung, and M. Z. Abdullah, "A novel 5.8 GHz array dielectric resonator antenna," *Progress In Electromagnetics Research C*, Vol. 15, 201–210, 2010.

7. Oliver, M. B., et al., "Circularly polarised rectangular dielectric resonator antenna," *Electronics Letters*, Vol. 31, No. 6, 418–419, 1995.
8. Kishk, A. A., "An elliptic dielectric resonator antenna designed for circular polarization with single feed," *Microwave and Optical Technology Letters*, Vol. 37, No. 6, 454–456, 2003.
9. Leung, K. W., et al., "Circular-polarised dielectric resonator antenna excited by dual conformal strips," *Electronics Letters*, Vol. 36, No. 6, 484–486, 2000.
10. Huang, C.-Y., J.-Y. Wu, and K.-L. Wong, "Cross-slot-coupled microstrip antenna and dielectric resonator antenna for circular polarization," *IEEE Transactions on Antennas and Propagation*, Vol. 47, No. 4, 605–609, 1999.
11. Li, B., K. K. So, and K. W. Leung, "A circularly polarized dielectric resonator antenna excited by an asymmetrical U-slot with a backing cavity," *IEEE Antennas and Wireless Propagation Letters*, Vol. 2, No. 1, 133–135, 2003.
12. Hsiao, F.-R., T.-W. Chiou, and K.-L. Wong, "Circularly polarized low-profile square dielectric resonator antenna with a loading patch," *Microwave and Optical Technology Letters*, Vol. 31, No. 2, 157–159, 2001.
13. Laisne, A., R. Gillard, and G. Piton, "Circularly polarised dielectric resonator antenna with metallic strip," *Electronics Letters*, Vol. 38, No. 2, 106–107, 2002.
14. Petosa, A., A. Ittipiboon, and M. Cuhaci, "Array of circular-polarised cross dielectric resonator antennas," *Electronics Letters*, Vol. 32, No. 19, 1742–1743, 1996.
15. Kishk, A. A., "Performance of planar four-element array of single-fed circularly polarized dielectric resonator antenna," *Microwave and Optical Technology Letters*, Vol. 38, No. 3, 381–384, 2003.
16. Palmer, K. D., J. H. Cloete, and J. J. van Tonder, "Bandwidth improvement of circularly polarised arrays using sequential rotation," *1992 Digest, Antennas and Propagation Society International Symposium, AP-S., Held in Conjunction with: IEEE URSI Radio Science Meeting and Nuclear EMP Meeting*, 1992.
17. Pang, K. K., et al., "Circularly polarized dielectric resonator antenna subarrays," *Microwave and Optical Technology Letters*, Vol. 27, No. 6, 377–379, 2000.
18. Haneishi, M. and H. Takazawa, "Broadband circularly polarised planar array composed of a pair of dielectric resonator antennas," *Electronics Letters*, Vol. 21, No. 10, 437–438, 1985.

19. Petosa, A., et al., "Bandwidth improvement for a microstrip-fed series array of dielectric resonator antennas," *Electronics Letters*, Vol. 32, No. 7, 608–609, 1996.
20. Mousavi Kejani, E. and M. H. Neshati. "Design investigation of circularly polarized Dielectric Resonator Antenna array excited by Dielectric Image Line," *2010 18th Iranian Conference on Electrical Engineering (ICEE)*, 2010.
21. Pozar, D. M., "Microstrip antenna aperture-coupled to a microstripline," *Electronics Letters*, Vol. 21, No. 2, 49–50, 1985.
22. Oliver, M. B., R. K. Mongia, and Y. M. M. Antar, "A new broadband circularly polarized dielectric resonator antenna," *1995 Digest, Antennas and Propagation Society International Symposium, AP-S.*, 1995.
23. Pozar, D., "A reciprocity method of analysis for printed slot and slot-coupled microstrip antennas," *IEEE Transactions on Antennas and Propagation*, Vol. 34, No. 12, 1439–1446, 1986.
24. Sullivan, P. and D. Schaubert, "Analysis of an aperture coupled microstrip antenna," *IEEE Transactions on Antennas and Propagation*, Vol. 34, No. 8, 977–984, 1986.
25. Ittipiboon, A., et al., "Aperture fed rectangular and triangular dielectric resonators for use as magnetic dipole antennas," *Electronics Letters*, Vol. 29, No. 23, 2001–2002, 1993.
26. Ruan, Y.-F., Y.-X. Guo, and X.-Q. Shi, "Equivalent circuit model of a tri-resonance wideband dielectric resonator antenna," *Microwave and Optical Technology Letters*, Vol. 49, No. 6, 1427–1433, 2007.
27. Kishk, A. A., et al., "Numerical analysis of stacked dielectric resonator antennas excited by a coaxial probe for wideband applications," *IEEE Transactions on Antennas and Propagation*, Vol. 51, No. 8, 1996–2006, 2003.
28. Collin, R. E., *Foundations for Microwave Engineering [Hauptw.]*, 2nd Edition, MacGraw-Hill, New York, 1992.
29. Kajfez, D. and P. Guillon, *Dielectric Resonators*, Artech House, Dedham, MA, 1986.
30. Mirshekar-Syahkal, D., *Spectral Domain Method for Microwave Integrated Circuits*, Research Studies Press, Wiley, New York, Taunton, Somerset, England, 1990.
31. Akhavan, H. G. and D. Mirshekar-Syahkal, "Approximate model for microstrip fed slot antennas," *Electronics Letters*, Vol. 30, No. 23, 1902–1903, 1994.